Model-based Design of Voltage Phase Controller for SPMSM in Field-weakening Region

Takayuki Miyajima and Hiroshi Fujimoto
The University of Tokyo
Kashiwa, Chiba, Japan
miya@fujilab.k.u-tokyo.ac.jp, fujimoto@k.u-tokyo.ac.jp

Masami Fujitsuna
DENSO CORPORATION
Kariya, Aichi, Japan
MASAMI_FUJITSUNA@denso.co.jp

***Abstract*— This paper investigates the nonlinear characteristic between voltage phase and torque and proposes a model-based design of voltage phase controller. PMSM drive systems should realize a quick torque response and have a wide operating range. However, in high-speed region, the control input is voltage phase only and the plant is nonlinear due to the inverter output voltage amplitude saturation. Because of this nonlinear characteristic between current and voltage phase, model-based design have not yet been carried out. As basic study, this paper proposes a model-based voltage phase controller for SPMSM. Simulation results and experimental results show the effectiveness of the model-based design method. In addition, the analysis of the derived plant model shows the relationship between q-axis current and voltage phase is a non-minimum phase system.**

I. INTRODUCTION

PMSMs (Permanent Magnet Synchronous Motors) are widely employed in many industrial applications because of high efficiency and high power density. Interior PMSMs (IPMSMs) are used in driven systems of electric vehicles, hybrid electric vehicles. Surface PMSMs (SPMSMs) are used for electric power steering systems. In these applications, the inverter output voltage is limited by the volume of the installed battery pack. Therefore, in order to achieve quick torque response under the voltage saturation, high performance PMSM control scheme is required.

Feedforward control methods based on model predictive control [1]–[3] have been proposed. The model-predictive control determines control input which optimizes the defined cost function such as torque tracking error. It can easily consider the voltage limit. The authors proposed feedforward field-weakening control method based on the final-state control [4]. However, feedforward control does not guarantee robustness to parameter variation. Thus, robust feedback control method is necessary. The voltage limiter methods [5], [6] operate current controller output so as to quicken its response. During this operation, the current feedback loop becomes an open-loop. The modulation feedback methods [7]–[9] cannot achieve quick torque response because it has two feedback loops.

During field-weakening control, the voltage amplitude is fixed and the control input is the voltage phase only. The voltage phase control [10], [11] operates voltage phase directly to compensate torque tracking error. However, the controller gains are determined by trial and error because of its nonlinear characteristics. This nonlinearcharacteristic has not been discussed precisely. In induction motors, transfer function between voltage phase and q-axis current had been analyzed [12], [13]. However it focused only on resonance peak of linearized transfer function in order to design the torque reference filter of modulation feedback system.

In this paper, a precise model-based design of voltage phase controller is proposed. This paper considers SPMSM for basic study. The precise plant model is derived based on linearization to use in the model-based design. An analysis of the proposed plant model shows that the plant is a non-minimum phase system during motor mode. A non-minimum phase system is the system whose zero is unstable [14]. Feedback control systems of a non-minimum phase system have the trade-off between undershoot and settling time. This trade-off is an achievable performance limitation of voltage phase control. The proposed model-based design method selects a PID controller as voltage phase controller in order to place all closed-loop poles to arbitrary values but these poles are slower than a unstable zero of the plant. Finally, simulations and experiments are performed to show the advantages of the proposed methods.

II. MODEL AND LINEARIZATION

A. dq Model of SPMSM

The voltage equations of SPMSM are represented by

$$\dot{\boldsymbol{x}}(t) = \begin{bmatrix} -\frac{R}{L} & \omega_e \\ -\omega_e & -\frac{R}{L} \end{bmatrix} \boldsymbol{x}(t) + \begin{bmatrix} \frac{v_d(t)}{L} \\ \frac{v_q(t) - \omega_e K_e}{L} \end{bmatrix}, \\ = \boldsymbol{f}(\boldsymbol{x},\ \boldsymbol{u}) \tag{1}$$

$$v_d(t) = -V_a(t)\sin\delta(t), \quad v_q(t) = V_a(t)\cos\delta(t), \tag{2}$$

$$\boldsymbol{x}(t) := [i_d(t) \quad i_q(t)], \quad \boldsymbol{u}(t) := [V_a(t) \quad \delta(t)], \tag{3}$$

where v_d, v_q, i_d, and i_q are the d- and q-axis voltages and currents, , L is the inductance, R is the stator winding resistance, ω_e is the electric angular velocity, K_e is the back EMF constant, V_a is the voltage amplitude, and δ is the voltage phase.

The torque T is described as

$$T(t) = K_{mt} i_q(t), \tag{4}$$

where $K_{mt} := PK_e$ and P is the number of pole pairs. In this paper, the 2-phase/3-phase transform is absolute transformation.

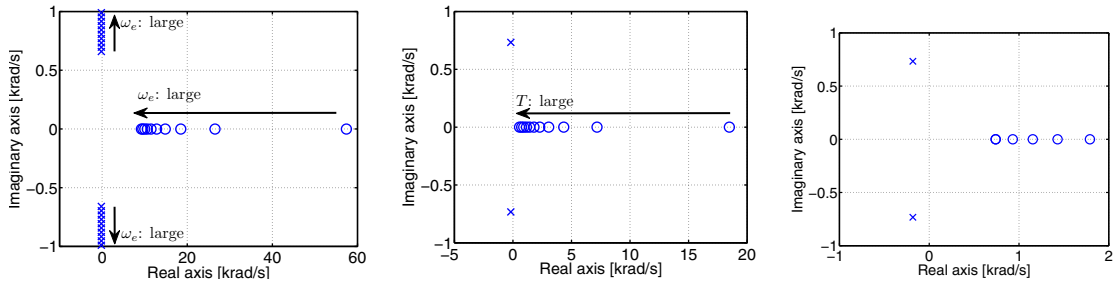

(a) Speed varies (b) Torque varies (c) Torque varies (zoom)

Fig. 1. A zero and poles of $\Delta P_{22}(s)$ in field-weakening region

B. Linearization

In field-weakening region, the manipulated variable is the voltage phase only. Therefore, the control system design is difficult due to the nonlinear characteristic between the voltage phase and the q-axis current (torque) as shown in (1). Thus, the voltage equation of SPMSM is linearized for model-based design.

Consider the equilibrium point $(\boldsymbol{x}_o,\ \boldsymbol{u}_o)$ which satisfies $\boldsymbol{f}(\boldsymbol{x}_o,\ \boldsymbol{u}_o) = 0$, where $\boldsymbol{u}_o = [V_{ao} \quad \delta_o]^T$ and $\boldsymbol{x}_o = [i_{do} \quad i_{qo}]^T$. (1) can be linearized around this equilibrium point by using first-order Taylor series as follows:

$$\frac{\mathrm{d}}{\mathrm{d}t}\begin{bmatrix}\Delta i_d\\ \Delta i_q\end{bmatrix} = \boldsymbol{A}\begin{bmatrix}\Delta i_d\\ \Delta i_q\end{bmatrix} + \boldsymbol{B}\begin{bmatrix}\Delta V_a\\ \Delta\delta\end{bmatrix}, \tag{5}$$

$$\boldsymbol{A} := \left.\frac{\partial \boldsymbol{f}}{\partial \boldsymbol{x}}\right|_{(\boldsymbol{x}_o,\boldsymbol{u}_o)} = \begin{bmatrix}-\frac{R}{L} & \omega_e\\ -\omega_e & -\frac{R}{L}\end{bmatrix}, \tag{6}$$

$$\boldsymbol{B} := \left.\frac{\partial \boldsymbol{f}}{\partial \boldsymbol{u}}\right|_{(\boldsymbol{x}_o,\boldsymbol{u}_o)} = \begin{bmatrix}-\frac{1}{L}\sin\delta_o & -\frac{V_{ao}}{L}\cos\delta_o\\ \frac{1}{L}\cos\delta_o & -\frac{V_{ao}}{L}\sin\delta_o\end{bmatrix}, \tag{7}$$

$$\Delta i_d := i_d - i_{do}, \quad \Delta i_q := i_q - i_{qo},$$
$$\Delta V_a := V_a - V_{ao}, \quad \Delta\delta := \delta - \delta_o.$$

The transfer functions from the voltage amplitude and the voltage phase to the d- and q-axis currents are obtained by

$$\begin{bmatrix}\Delta i_d\\ \Delta i_q\end{bmatrix} = \begin{bmatrix}\Delta P_{11}(s) & \Delta P_{12}(s)\\ \Delta P_{21}(s) & \Delta P_{22}(s)\end{bmatrix}\begin{bmatrix}\Delta V_a\\ \Delta\delta\end{bmatrix}, \tag{8}$$

$$\Delta P_{11}(s) = \frac{-\frac{1}{L}\sin\delta_o\left\{s + \frac{R}{L} - \omega_e\tan\left(\frac{\pi}{2} - \delta_o\right)\right\}}{s^2 + 2\frac{R}{L}s + \frac{R^2}{L^2} + \omega_e^2}, \tag{9}$$

$$\Delta P_{12}(s) = \frac{-\frac{V_{ao}}{L}\cos\delta_o\left(s + \frac{R}{L} + \omega_e\tan\delta_o\right)}{s^2 + 2\frac{R}{L}s + \frac{R^2}{L^2} + \omega_e^2}, \tag{10}$$

$$\Delta P_{21}(s) = \frac{\frac{1}{L}\cos\delta_o\left(s + \frac{R}{L} + \omega_e\tan\delta_o\right)}{s^2 + 2\frac{R}{L}s + \frac{R^2}{L^2} + \omega_e^2}, \tag{11}$$

$$\Delta P_{22}(s) = \frac{-\frac{V_{ao}}{L}\sin\delta_o\left\{s + \frac{R}{L} - \omega_e\tan\left(\frac{\pi}{2} - \delta_o\right)\right\}}{s^2 + 2\frac{R}{L}s + \frac{R^2}{L^2} + \omega_e^2}, \tag{12}$$

The proposed model-based design method for voltage phase controller uses $\Delta P_{22}(s)$ which is the linear transfer function between q-axis current and voltage phase.

TABLE I

NOMINAL PARAMETERS UNDER THE TEST

R	33.7 [mΩ]
L	0.185 [mH]
K_e	11.60 [mV/(rad/s)]
P	7
dc-bus voltage V_{dc}	12.0 [V]
maximum modulation index $M_{\max}$	1.0

C. Analysis of linearized plant model

From the viewpoint of zeros, the characteristics of the transfer functions from voltage phase to d- and q-axis currents. The zeros of $\Delta P_{12}(s)$ and $\Delta P_{22}(s)$ are represented by (13) and (14), respectively.

$$z_{12} = -\frac{R}{L} - \omega_e\tan\delta_o. \tag{13}$$

$$z_{22} = -\frac{R}{L} + \omega_e\tan\left(\frac{\pi}{2} - \delta_o\right). \tag{14}$$

The poles are described by

$$p_1,\ p_2 = -\frac{R}{L} \pm j\omega_e \tag{15}$$

Namely, the poles and the zeros are functions of the operating point. In the field-weakening region, $\frac{R}{L} \ll \omega_e$. Therefore, during motoring mode ($0 < \delta_o < \pi$), $\Delta P_{12}(s)$ and $\Delta P_{22}(s)$ have a stable zero and a unstable pole, respectively. On the other hand, under regeneration ($-\pi < \delta_o < 0$), $\Delta P_{12}(s)$ and $\Delta P_{22}(s)$ have an unstable zero and a stable pole, respectively. The imaginary parts of poles is depend on the operating frequency.

Fig. 1(a) reports the values of a zero and poles when the speed varies from 900 [rpm] to 1400 [rpm] under 0 [Nm]. Here, Table I illustrates the nominal parameters of the test. The zero is unstable. By increasing motor speed, the zero slows because the voltage phase increases in field-weakening region.

Fig. 1(b) illustrates the characteristic between the zero and the torque when the torque is changed from 0 [Nm] to 3 [Nm] at 1000 [rpm]. Increment of torque makes unstable zero slow. In high-torque region, the zero is extremely slow as shown Fig. 1(c). This slow unstable zero makes a trade-off between quick torque response and small undershoot.

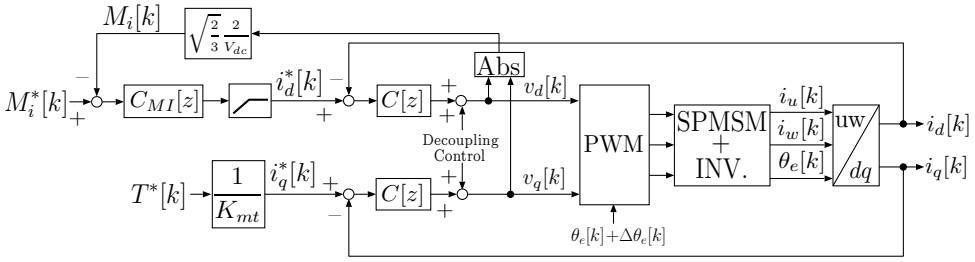

Fig. 2. The block diagram of the conventional method 1.

III. CONTROL SYSTEM DESIGN

The proposed method is compared with two conventional methods. The conventional method 1 is the modulation feedback control. The conventional method 2 consists of the current vector control, the voltage phase control which is designed by trial and error, and the control switch structure. On the other hand, the proposed method designs voltage phase controller by model-based design. Briefly, the difference between the conventional method 2 and the proposed method is the design of voltage phase controller only.

A. Conventional method 1: modulation feedback control

Fig. 2 shows the block diagram of the conventional method 1. The conventional method 1 has two feedback loops: current loop and modulation index loop.

In the current loop, the coupling terms in (1) are rejected by the decoupling controls which are represented by

$$v_d[k] = v'_d[k] - \omega_e[k]Li_q[k], \tag{16}$$

$$v_q[k] = v'_q[k] + \omega_e[k](Li_d[k] + K_e), \tag{17}$$

where v'_d and v'_q denote the d- and q- axis current feedback controller outputs, respectively.

The d- and q-axis current feedback controllers are designed to be a plant-pole cancellation feedback control as follow:

$$C(s) = \frac{Ls + R}{\tau s}, \quad \tau = 1.0 \text{ [ms]}, \tag{18}$$

where τ is the selected bandwidth of the current loop. The discretized controller $C[z]$ by the Tustin transform is applied to the control system.

In the modulation index loop, the modulation index controller $C_{MI}[z]$ which is PI controller obtains the d-axis current reference $i_d^*[k]$ to put the current references within the voltage limit circle. In this paper, the gains of $C_{MI}(s)$ are designed as the proportional gain and the integral gain are 10 and 100, respectively, by trial and error. By discretizing $C_{MI}(s)$, $C_{MI}[z]$ is obtained by Tustin transformation with T_u.

B. Conventional method 2: voltage phase controller is designed by trial and error

If the voltage amplitude is not saturated, the conventional method 2 applies current vector control to the control system. On the other hand, at the operating point on the voltage limit circle, the torque is controlled with the voltage phase controller.

1) Current vector control: The block diagram of current feedback control is described in Fig. 3. The current feedback controller $C[z]$ and the decoupling control are the same with the conventional method 1.

When the voltage reference is saturated before switching to the voltage phase control, it is limited as

$$\tilde{\boldsymbol{V}}_a[k] = \begin{cases} \dfrac{\boldsymbol{V}_a[k]}{|\boldsymbol{V}_a[k]|} V_{a\max} & (|\boldsymbol{V}_a[k]| > V_{a\max}) \\ \boldsymbol{V}_a[k] & (\text{otherwise}) \end{cases} \tag{19}$$

where $\boldsymbol{V}_a = [v_d \;\; v_q]^T$, $\tilde{\boldsymbol{V}}_a$ is the limited voltage reference, and $V_{a\max}(:= \sqrt{3/2}M_{\max}V_{dc})$ is the maximum voltage amplitude. Here, $\sqrt{3/2}$ is the coefficient to transform two-phase into three-phase. Under voltage amplitude saturation, an anti-windup control in [15] is applied.

2) Voltage phase control [10]: The conventional voltage phase controller reported in Fig. 4(a) uses a PI controller which is expressed as

$$C_{\delta PI} = \frac{K_P s + K_I}{s}, \tag{20}$$

where K_I and K_P are the integral and proportional gains. These gains are determined by trial and error so that the transient response becomes small damped oscillation. The control gains are $K_P = 0.0001$ and $K_I = 2$. By discretizing with Tustin transform, $C_{\delta PI}[z]$ is obtained.

During the voltage phase control, constant voltage amplitude $V_{a\max}$ is given.

3) Control switch structure: When the voltage amplitude is limited in transient response, d-axis current and q-axis current cannot track the reference. Therefore, The switching condition from the current vector control to the voltage phase control is based on d-axis current error. If the absolute value of d-axis current error which is represented by (21) exceeds the baseline X_1, the mode of controller is changed from the current vector control to the voltage phase control. At this point, state variables of voltage phase controller is compensated with the current feedback controller outputs.

$$Y_1[k] \;\; = \;\; \begin{cases} i_d^* - i_d + Y_1[k-1] & (V_a \geq V_{a\max}) \\ 0 & (\text{otherwise}) \end{cases} \tag{21}$$

On the other hand, the switching condition from the voltage phase control to the current vector control is based on the value of d-axis current. If $i_d > 0$, the torque reference

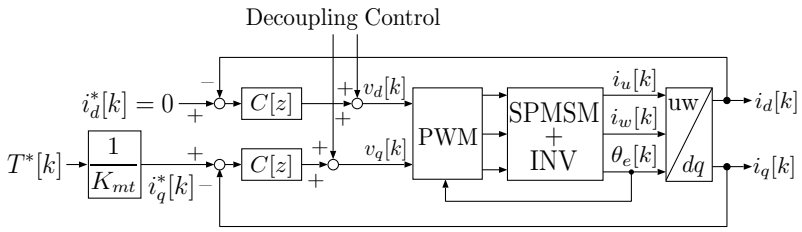

Fig. 3. Block diagram of the current vector control (conventional method 2 and proposed method).

can be achieved by the current vector control. Therefore, the control system is switched to the current vector control. (22) expresses the sum of the d-axis current under smaller q-axis current tracking error than X_2. If Y_2 is smaller than the baseline X_3, the voltage phase controller is applied to the control system. At this point, state variables of $C[z]$ is compensated with the d-axis and q-axis voltages.

$$Y_2[k] = \begin{cases} i_d[k] + Y_2[k-1] & (|i_q^* - i_q| \le X_2) \\ 0 & (\text{otherwise}) \end{cases} \quad (22)$$

X_1, X_2, and X_3 are determined by trial and error. In this paper, they are selected as $X_1 = 100$, $X_2 = 1$, and $X_3 = 40$.

C. Proposed method: Model-based voltage phase control

The current vector control and control the switch structure of the proposed method are the same as the conventional method 2 but the design method of voltage controller is different. The proposed method designs voltage phase controller with model-based design. Fig. 4(b) represents the block diagram of model-based voltage phase control.

The voltage phase controller $C_{\delta PID}[z]$ is designed with the linearized plant model $\Delta P_{22}(s)$. However, this model is linearized around an equilibrium point. Here, the voltage phase controller is used during the voltage amplitude saturation. Thus, the equilibrium point is an intersection of the voltage limit circle and the torque constant line. The voltage phase on this intersection can be determined from the q-axis current reference i_q^* uniquely as follows:

$$\delta_o[k] = \sin^{-1}\left\{\frac{\left(R^2+\omega_e^2L^2\right)i_q^*[k] + \omega_e K_e R}{\sqrt{R^2+\omega_e^2L^2}V_{a\max}}\right\} - \tan^{-1}\frac{R}{\omega_e L}. \quad (23)$$

In this paper, in order to place all close-loop poles at arbitrary values, the authors selected a PID controller as the voltage phase controller. By using the linearized plant model $\Delta P_{22}(s)$ on the equilibrium point ($V_{a\max}$, δ_o), $C_{\delta PID}(s)$ is designed by pole placement. However, in high-speed region, the plant has fast complex conjugate poles. All closed-loop poles should be faster than the plant poles. However, fast closed-loop poles cause undershoot because the plant is a non-minimum phase system. Therefore, at the high-speed region, the proposed method places all closed-loop poles on a circle which goes through the plant poles and has a center at the origin. In this paper, the real parts of all close-loop poles are placed at -750 [rad/s]. $C_\delta[z]$ is

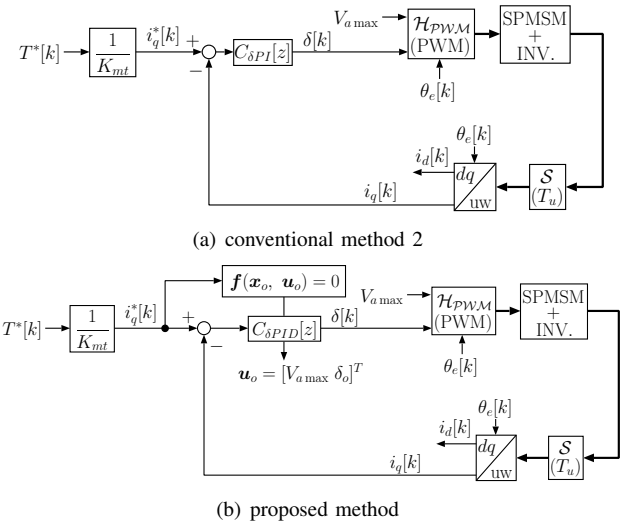

(a) conventional method 2

(b) proposed method

Fig. 4. Block diagram of the voltage phase control.

obtained by Tustin transformation with control period T_u. Here, the parameters of $\Delta P_{22}(s)$ vary depending on the operating point, namely, the proposed model-based voltage phase controller is a variable gain controller.

IV. Simulation

The proposed method is evaluated firstly by simulation results. The parameters under simulations are the same as Table I. The sampling period T_u is 0.1 [ms].

Fig. 5, Fig. 6, and Fig. 7 show step torque responses at 800 [rpm]. Here, the "SW" represents the mode of controller. When the SW is "high", the voltage phase control is applied. On the other hand, the current vector control is applied when the SW is "low". The conventional method 1 has the current loop and the modulation index loop. The modulation loop is the outer of the current feedback loop which has low bandwidth due to voltage saturation. Therefore, it cannot achieve quick current response. On the other hand, after switching to voltage phase control, The conventional method 2 and the proposed method realize quicker current response in comparison with the conventional method 1. However, the gains of the conventional method 2 are small for small damped oscillation. As a result, current response is slow. The proposed method designs high-bandwidth voltage phase controller with precise plant model. It achieves quickest current response.

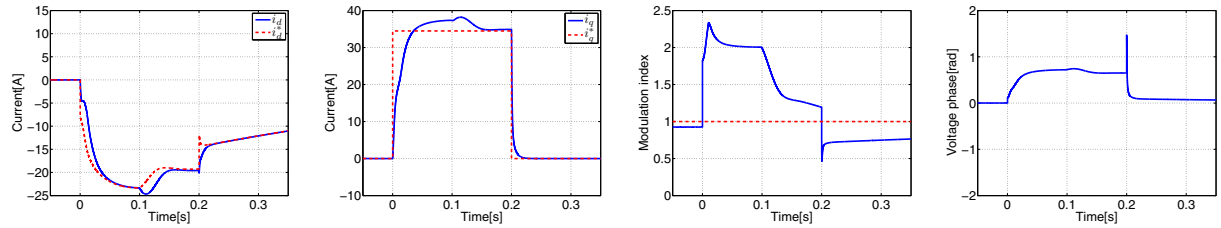

(a) d-axis current i_d (b) q-axis current i_q (c) Modulation index (d) Voltage phase δ

Fig. 5. Simulation result (800 [rpm], conventional method 1).

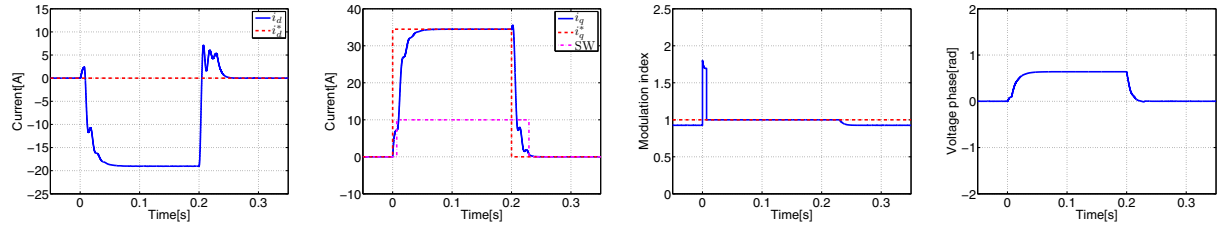

(a) d-axis current i_d (b) q-axis current i_q (c) Modulation index (d) Voltage phase δ

Fig. 6. Simulation result (800 [rpm], conventional method 2).

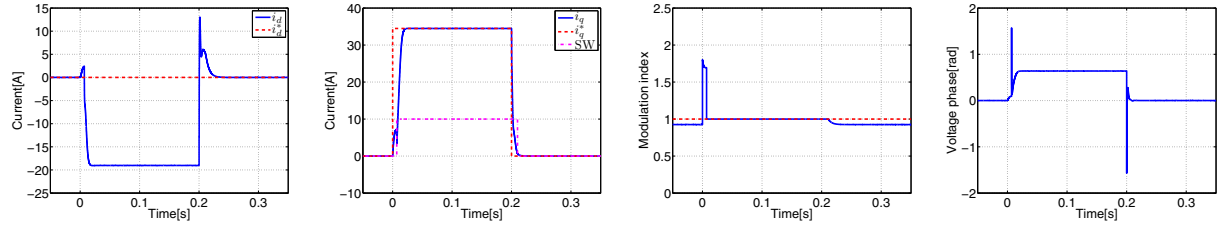

(a) d-axis current i_d (b) q-axis current i_q (c) Modulation index (d) Voltage phase δ

Fig. 7. Simulation result (800 [rpm], proposed method).

Fig. 8, Fig. 9, and Fig. 10 describe step torque responses at 1000 [rpm]. According to this simulation, torque is controlled by voltage phase controller only.

Both conventional methods cannot achieve quick current response. In contrast, the proposed method shortens the setting time.

V. EXPERIMENT

Experiments were conducted under the same condition as simulations. In the conventional method 1, d-aix current reference is limited within -80 [A] to avoid the divergence of the modulation index loop.

Fig. 11, Fig. 12, and Fig. 13 reports step torque responses at 800 [rpm]. Current responses in the conventional method 1 is very slow because the modulation index loop has a cascaded feedback systems. The conventional method 2 cannot quick response because it is designed by trial and error. On the other hand, the proposed method achieves quick current response owing to the precise model-based design.

The experimental results at 1000 [rpm] are shown in Fig. 14, Fig. 15 and Fig. 16. The proposed method controls q-axis current quickly. The proposed design method realizes high performance.

VI. CONCLUSION

In order to achieve high bandwidth control under voltage saturation, this paper proposes a precise model-based design of voltage phase controller for SPMSM. For the model-based design of voltage phase controller, the voltage equation of SPMSM is linearized. Detailed analysis of the proposed precise plant model shows that the relationship between q-axis current and voltage phase is a non-minimum phase system depending on the operating point. The simulation results and experimental results verified the effectiveness of the proposed design method.

In our future works, the authors will apply this proposed theory to IPMSMs.

ACKNOWLEDGMENT

This research was partly supported by the Ministry of Education, Culture, Sports, Science and Technology grant No. 22246057.

REFERENCES

[1] P. Vaclavek and P. Blaha: “Model based High-performance PMSM Drive Control”, SICE Annual Conference 2010, pp.227–232, 2010.

[2] T. Geyer: “Computationally Efficient Model Predictive Direct Torque Control”, IEEE Trans. Power Electronics, Vol. 26, No. 10, pp. 2804–2816, 2011.

[3] T. Maeda and S. Doki: “Improvement of Torque Control System of PMSM based on Model Predictive Control”, 37th Annual Conference on IEEE Industrial Electronics Society, pp. 1891–1896, 2011.

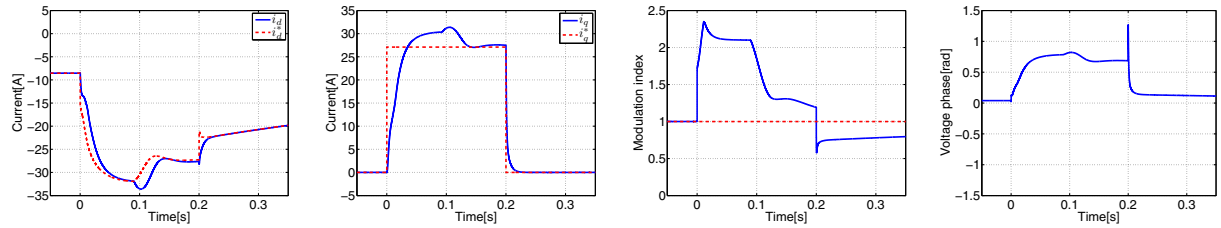

(a) d-axis current i_d (b) q-axis current i_q (c) Modulation index (d) Voltage phase δ

Fig. 8. Simulation result (1000 [rpm], conventional method 1).

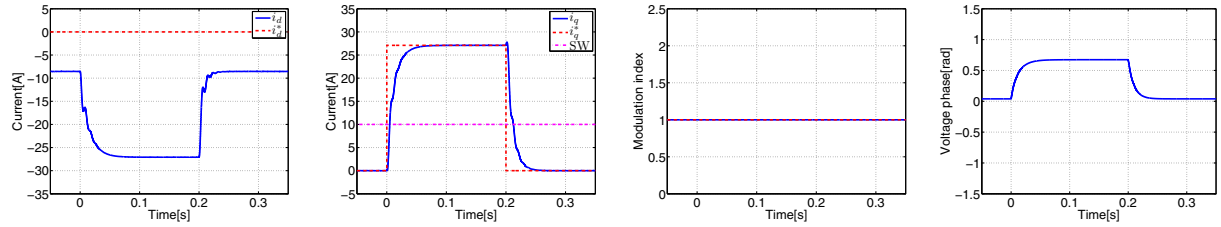

(a) d-axis current i_d (b) q-axis current i_q (c) Modulation index (d) Voltage phase δ

Fig. 9. Simulation result (1000 [rpm], conventional method 2).

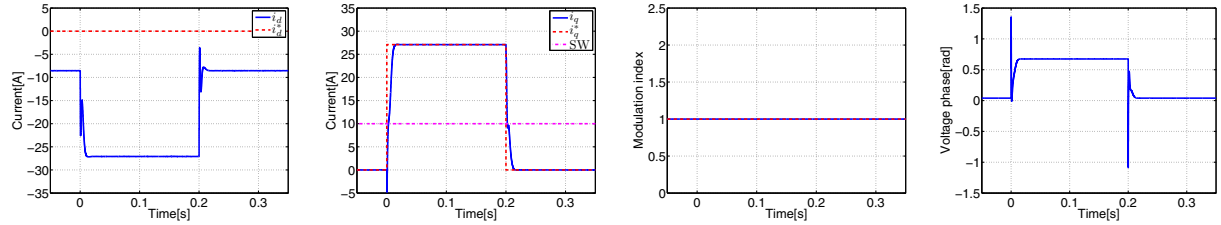

(a) d-axis current i_d (b) q-axis current i_q (c) Modulation index (d) Voltage phase δ

Fig. 10. Simulation result (1000 [rpm], proposed method).

[4] T. Miyajima, H. Fujimoto, and M. Fujitsuna: "Feedforward control for SPMSM with Final State Control Based on Voltage Limit Circle with Transient Term", The 2011 IEEE Energy Conversion Congress and Exposition, pp.3913–3919, 2011.

[5] B.-H. Bae and S.-K. Sul: "A Novel Dynamic Overmodulation Strategy for Fast Torque Control of High-Saliency-Ratio AC Motor", IEEE Trans. Ind. Appl., Vol.41, No.4, pp.1013–1019, 2005.

[6] S. Lerdudomsak, S. Doki, and S. Okuma: "Voltage Limiter Calculation Method for Fast Torque Response of IPMSM in Overmodulation Range", The 35th Annual Conference of the IEEE Industrial Electronics Society, pp. 1385–1390, 2009.

[7] K. Kondo, K. Matsuoka, Y. Nakazawa, and H. Shimizu: "Torque feedback control for salient pole permanent magnet synchronous motor at weakening flux control range", T.IEEJapan, Vol. 119-D, No. 10, pp. 1155–1164, 1999 (in Japanese).

[8] T.-S. Kwon, G.-Y. Choi, M.-S. Kwak, and S.-K Sul : "Novel Flux-Weakening Control of an IPMSM for Quasi-Six-Step Operation", IEEE Trans. Ind. Appl., Vol. 44, NO. 6, pp. 1722–1723, 2008.

[9] H. Liu, Z. Q. Zhu, E. Mohamed, Y. Fu, and X. Qi: "Flux-Weakening Control of Nonsalient Pole PMSM Having Large Winding Inductance, Accounting for Resistive Voltage Drop and Inverter Nonlinearities", IEEE Trans. Power Electronics, Vol. 27, No. 2, pp. 942–952, 2012.

[10] H. Nakai, H. Ohtani, E. Satoh, and Y. Inaguma: "Development and Testing of the Torque Control for the Permanent-Magnet Synchronous Motor", IEEE Trans. Ind. Electron., Vol. 52, No. 3, pp. 800–806, 2005.

[11] W. Hatsuse, Y. Notohara, K. Ohi, K. Tobari, K. Tamura, C. Unoko, and Y. Iwaji: "A Stable Field-Weakening Control Using Voltage Phase Operations in the High-Power Region", The 2010 International Power Electronics Conference, pp.599–604, 2010.

[12] Y. Nakazawa, S. Toda I. Yasuoka, and H. Naito: "One-Pulse PWM Mode Vector Control for Traction Drives", IEEE Power Electronics in Transportation, pp. 135–141, 1996.

[13] Y. Nakazawa, S. Toda, and I. Yasuoka: "A New Vector Control for Induction. Motor Drives in Full Block Mode of Inverters", T.IEEJapan, Vol. 119-D, No. 9, pp. 1071–1080, 1998 (in Japanese).

[14] J. B. Hag and D. S. Bernstein: "Nonminimum-phase zeros - much to do about nothing - classical control - revisited part II", IEEE Control system magazine, Vol. 27, No. 3, pp. 45–57, 2006.

[15] K. Ohishi, E. Hayasaka, T. Nagano, and H. Masaya: "High-performance speed servo system considering Voltage saturation of a vector-controlled induction motor", IEEE Trans. Ind. Electron., Vol. 5., NO. 3, pp. 795–802, 2006.

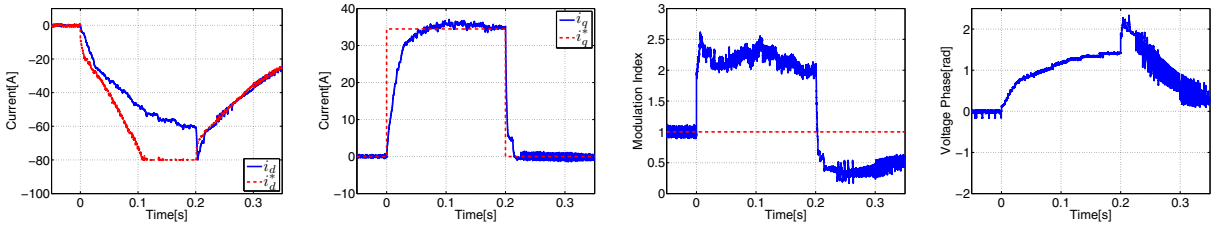

(a) d-axis current i_d (b) q-axis current i_q (c) Modulation index (d) Voltage phase δ

Fig. 11. Experimental result (800 [rpm], conventional method 1).

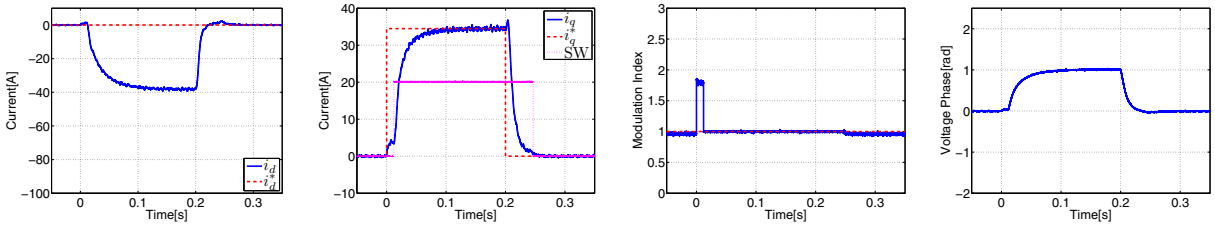

(a) d-axis current i_d (b) q-axis current i_q (c) Modulation index (d) Voltage phase δ

Fig. 12. Experimental result (800 [rpm], conventional method 2).

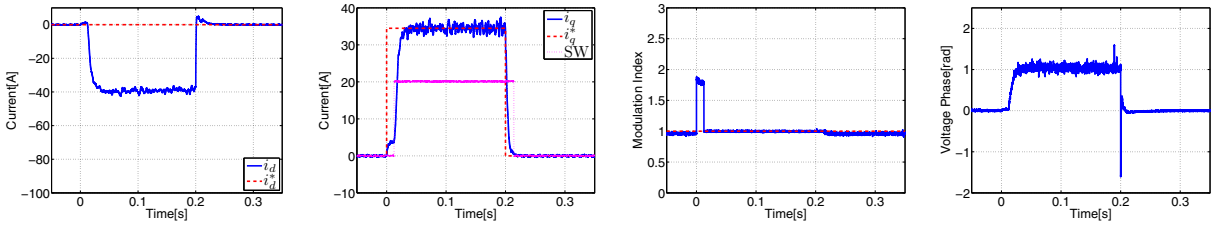

(a) d-axis current i_d (b) q-axis current i_q (c) Modulation index (d) Voltage phase δ

Fig. 13. Experimental result (800 [rpm], proposed method).

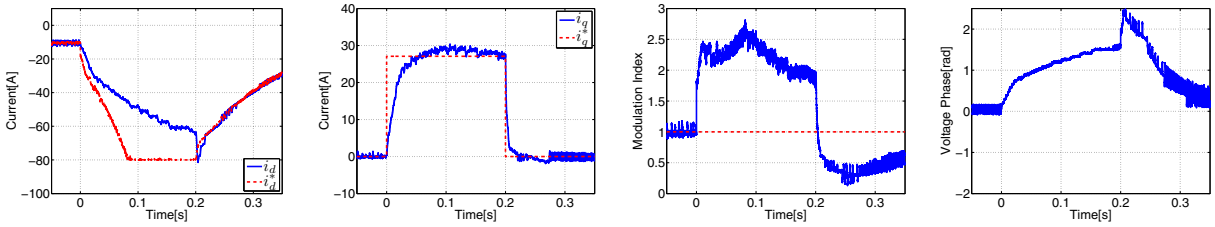

(a) d-axis current i_d (b) q-axis current i_q (c) Modulation index (d) Voltage phase δ

Fig. 14. Experimental result (1000 [rpm], the conventional method).

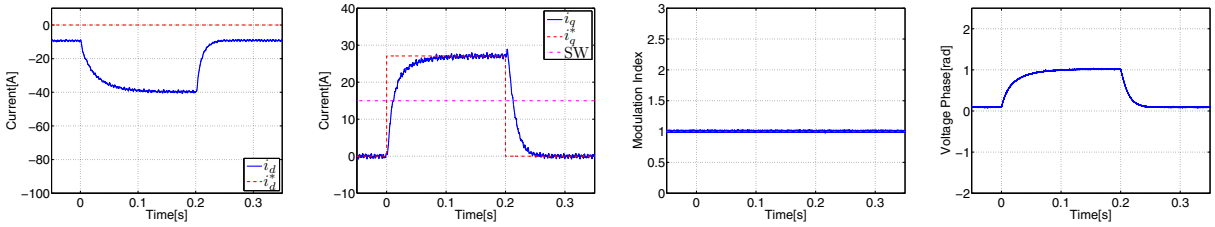

(a) d-axis current i_d (b) q-axis current i_q (c) Modulation index (d) Voltage phase δ

Fig. 15. Experimental result (1000 [rpm], conventional method 2).

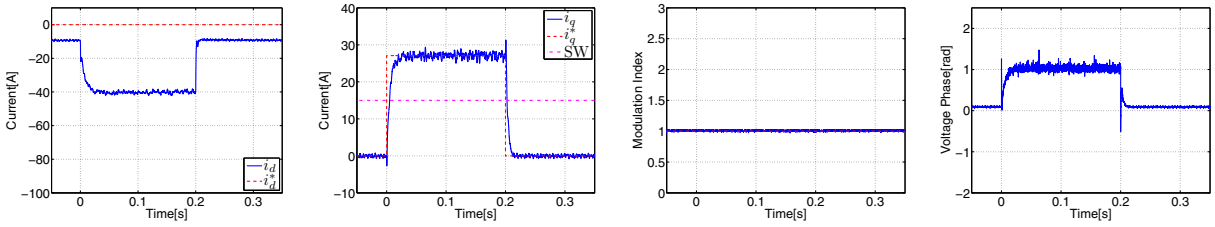

(a) d-axis current i_d (b) q-axis current i_q (c) Modulation index (d) Voltage phase δ

Fig. 16. Experimental result (1000 [rpm], proposed method).